Range-angle Decoupled Transmit Beamforming with Frequency Diverse Array

Xiang Zhe Chen Baixiao*

(*National Laboratory of Radar Signal Processing, Xidian University, Xi'an* 710071, *China*)

Abstract: It has been shown that Frequency Diverse Arrays (FDA) exhibit a range-angle dependent beam steering feature by employing a uniform frequency increment across the array elements. However, this beam pattern generates maxima at multiple range values, possibly leading to loss of signal-to-interference-plus-noise ratio when the interferences are located at any of the maxima. Herein, we prove that the beam pattern of FDA is range-periodic and propose the basic criteria for the FDA configuration to decouple the range and angle. In an illuminated space, a single-maximum beam pattern can be obtained by configuring the frequency increment between the elements. Specific examples have been discussed herein, and the simulation results verify the proposed theory.

Key words: Frequency Diverse Arrays (FDA); Range-angle-dependent; Single-maximum beampattern; Configuration

DOI: 10.12000/JR16113

Reference format: Xiang Zhe and Chen Baixiao. Range-angle decoupled transmit beamforming with frequency diverse array[J]. *Journal of Radars*, 2018, 7(2): 212–219. DOI: 10.12000/JR16113.

引用格式：项喆, 陈伯孝. 频率分集阵列的距离角度解耦的波束形成[J]. 雷达学报, 2018, 7(2): 212–219. DOI: 10.12000/JR16113.

频率分集阵列的距离角度解耦的波束形成

项喆 陈伯孝

(西安电子科技大学雷达信号处理国家重点实验室 西安 710071)

摘 要：常规频率分集雷达(FDA)在发射阵元采用均匀的频率间隔，从而可以形成距离-角度耦合的波束方向图。但是该方向图在多个距离上均形成多峰值波束，当干扰位于任一波束最大指向的距离时，将会带来信干噪比损失。针对上述问题，该文通过分析波束形成的表达式，从原理上提出一个关于频率分集雷达阵列配置的基本原则，能够在指定的距离角度范围内，形成单峰值的波束方向图。几种特例和仿真结果均证明了该原则的有效性。

关键词：频率分集雷达；距离-角度耦合；单峰值波束；阵列配置

中图分类号：TN959.73; V243.2 **文献标识码：**A **文章编号：**2095-283X(2018)02-0212-08

1 Introduction

Frequency Diverse Arrays (FDA) radar has recently drawn much attention among the researchers. FDA differs from the traditional phased array by using a small frequency increment across the array elements, which results in a range-angle-dependent beam pattern. FDA radar system is first proposed in Ref. [1]. In FDA radar, a uniform interelement frequency offset is applied across the array elements. FDA radar with uniform small and large frequency offset frequency has been investigated in Refs. [1–7]. Small frequency offset has been exploited to generate range-dependent beampattern, while large frequency offset can get independent echoes from the target.

Manuscript received October 08, 2016; Revised January 20, 2017; Published online March 22, 2017.

Foundation Items: The National Natural Science Foundation of China (61571344), Shanghai Academy of Spaceflight Technology (SAST2015064, SAST2015071)

*Communication author: Chen Baixiao.

E-mail: bxchen@xidian.edu.cn.

Unlike the phased array, the range-angle dependency of the FDA beampattern allows the radar system to focus the transmit energy in a desired range-angle space. This unique feature of FDA helps to suppress the range-dependent interferences[8] and increases the received SINR consequently. Especially for the mainlobe interference and clutter, the FDA can achieve a significant improvement in SINR against the phased array because the FDA provides the increased Degrees Of Freedom (DOFs) in range domain. However, the FDA beampattern is shown to be periodic in range and time[2], which goes to maximum at multiple time and range values. With this multiple-maximum beampattern, the resulting SINR will be deteriorated when the interferers are located at any of the maxima. To improve SINR, FDA with Time-Dependent Frequency Offset (TDFO-FDA) was proposed to achieve a time-independent beampattern at the target location[9]. Nevertheless, the proposed beampattern is still periodic in range which will result in the loss of SINR. A nonuniformly spaced linear FDA with linear incremental frequency increment has also been studied in Ref. [10], and a nonrepeating beampattern has been obtained for range-angle imaging of targets. A uniformly spaced linear FDA with Logarithmically (Log-FDA) increasing frequency offset is proposed in Ref. [11]. The proposed strategy provides a nonperiodic beampattern with the single-maximum in space. In Ref. [12], the beampattern of FDA who transmits the pulsed signal has been studied. Lately, few more publications have done some work in decoupling the range-angle dependent beampattern of FDA[13–16]. All these papers only address the properties of the FDA beampattern, and they do not study the common rule for the FDA configuration to form a single-maximum transmit beampattern.

With the pioneer work on FDA radar, we aim to decouple the range and angle in the beampattern and provide a nonperiodic beampattern with the single-maximum in the illuminated range-angle space. In this paper, we propose a basic criteria for the FDA configuration, in which the element spacing and frequency increment are configurable, to form a single-maximum beampattern through mathematical analysis. This single-maximum beampattern, unlike the multiple-maxima beampattern, can help to further suppress range-dependent interferences, causing improved SINR and increased detect ability. The proposed rule for the FDA configuration will be helpful to design the FDA.

The rest of the paper is organized as follows. In Section 2, the basic FDA model has been described and the basic criterion is derived for the FDA configuration to form a single-maximum beampattern through mathematical analysis. Moreover, several specific conditions are introduced. In Section 3, the beampattern has been plotted for the specific conditions discussed in Section 2. Finally, in Section 4 we conclude the paper.

2 Design and Mathematical Analysis of FDA

2.1 System description

Consider an array of M transmit elements, we assume that the waveform radiated from each antenna element is identical with a frequency increment, as shown in Fig. 1. The radiated frequency from the m-th element is

$$f_m = f_0 + \Delta f_m,\ \ m = 0, \cdots, M-1 \tag{1}$$

where Δf_m is the frequency increment of m-th element with reference to the carrier frequency f_0. Specifically, $\Delta f_0 = 0$.

Considering a given far-field point, the phase of the signal transmitted by the m-th element can be represented by

$$\psi_m = 2\pi f_m \left(t - \frac{r_m}{\mathrm{c}}\right) \tag{2}$$

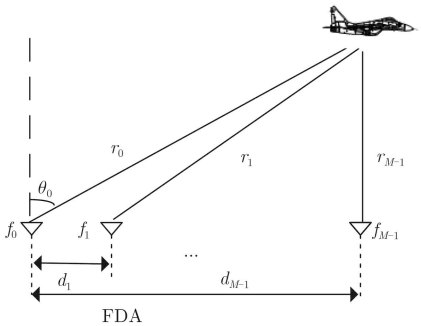

Fig. 1 FDA configuration

where c and r_m are the speed of light and the distance between the m-th element and the observed point, respectively.

The range difference between individual elements is approximated by

$$r_m = r_0 - d_m \sin\theta_0 \tag{3}$$

where θ_0 is the desired angle, d_m is the spacing between the m-th element and the first element. Specifically, $d_0 = 0$.

So the phase difference between the m-th element and the first element is

$$\begin{aligned}\Delta\psi_m &= \psi_m - \psi_0 = 2\pi\left(f_m\left(t - \frac{r_m}{\mathrm{c}}\right) - f_0\left(t - \frac{r_0}{\mathrm{c}}\right)\right)\\ &= 2\pi\Delta f_m t - 2\pi\frac{f_m d_m \sin\theta_0}{\mathrm{c}} + 2\pi\frac{\Delta f_m r_0}{\mathrm{c}}\end{aligned} \tag{4}$$

In Eq. (4), the third term is important because it shows that the FDA radiation pattern depends on both the range and the frequency increment. Taking the first element as the reference for the array, the steering vector can be expressed as

$$\boldsymbol{a}(\theta, r, t) = \left[1, \cdots, \exp\left(-\mathrm{j}2\pi \cdot \frac{-\Delta f_m(t\mathrm{c} + r) + f_m d_m \sin\theta}{\mathrm{c}}\right)\right]^{\mathrm{T}} \tag{5}$$

where $[\cdot]^{\mathrm{T}}$ denotes the transpose operator.

In the pusled-FDA, for $t \in \left[-\frac{T_\mathrm{e}}{2}, \frac{T_\mathrm{e}}{2}\right]$, T_e is the pulsewidth, the maximum value of phase variance[12] during the pulse duration can be derived as

$$\xi = \max_m 2\pi\Delta f_m T_\mathrm{e} \tag{6}$$

When the phase variance ξ is small enough, the beampattern of the pulsed-FDA can be viewed as quasi-static. Actually, in practical radar systems, duty cycle other than pulse duration is often used to describe the characterization of the pulsed-waveform. Then, the phase variance ξ can be further written as

$$|\xi| = \max_m 2\pi\frac{|\Delta f_m|}{f_r} d_t = 2\pi d_t \max_m \rho_m \ll 1 \tag{7}$$

where d_t is the duty cycle, which is usually small. Eq. (7) holds when $\max_m \rho_m$ is also small.

So under the condition Eq. (7), the time t can be neglected. So Eq. (5) can be simplified as

$$\boldsymbol{a}(\theta, r) = \left[1, \cdots, \exp\left(-\mathrm{j}2\pi \cdot \frac{-\Delta f_m r + f_m d_m \sin\theta}{\mathrm{c}}\right)\right]^{\mathrm{T}} \tag{8}$$

2.2 Transmit beampattern analysis

Throughout this paper, we assume a narrowband system where the propagation delays manifest as phase shifts to the transmitted signals and Eq. (7) is satisfied. To steer the maximum at an expected target location (θ_0, r_0), the complex weights are configured as $\boldsymbol{a}(\theta_0, r_0)$, so the transmit beampattern can be expressed

$$\begin{aligned}\mathrm{AF}(\theta, r) &= \left|\boldsymbol{a}^{\mathrm{H}}(\theta_0, r_0)\,\boldsymbol{a}(\theta, r)\right|\\ &= \left|\sum_{m=0}^{M-1}\exp\left(\mathrm{j}2\pi\frac{\Delta f_m(r - r_0) - f_m d_m(\sin\theta - \sin\theta_0)}{\mathrm{c}}\right)\right|\end{aligned} \tag{9}$$

where $[\cdot]^{\mathrm{H}}$ denotes the conjugate transpose operator.

It is easy to see that the beam direction will vary as a function of the range and angle, which means the beampattern is range-angle dependent. Since the beampattern is coupled in the range and angle, the target's range and angle cannot be estimated directly by the FDA beamformer output. Note that the beampattern is also related to Δf_m and d_m, so the desired single-maximum beampattern can be obtained by setting the proper Δf_m and d_m.

In Eq. (9), when $m = 0$, the exponential term is equal to 1. To obtain the maximum value of the beampattern, the exponential terms should be all equal to 1 for $m = 1, 2, \cdots, M-1$. So the phase of the exponential term should be the integral multiple of 2π, which can be expressed as

$$\frac{\Delta f_m(r - r_0) - f_0 d_m(\sin\theta - \sin\theta_0) - \Delta f_m d_m(\sin\theta - \sin\theta_0)}{\mathrm{c}} = L_m \tag{10}$$

where L_m is an integer, *e.g.* $L_m = 0, \pm1, \cdots$, $m = 1, 2, \cdots, M-1$.

The Eq. (10) can be rewritten as

$$r = \frac{L_m\mathrm{c} + f_0 d_m(\sin\theta - \sin\theta_0)}{\Delta f_m} + d_m(\sin\theta - \sin\theta_0) + r_0 \tag{11}$$

Since $d_m(\sin\theta - \sin\theta_0) \ll r_0$, the term $d_m(\sin\theta - \sin\theta_0)$ in Eq. (8) can be neglected. The curves

formed by Eq. (11) will be called as range-angle distribution curves throughout the paper. Then Eq. (11) can be approximately expressed as

$$\begin{aligned}&\Delta f_m(r-r_0)-f_0 d_m(\sin\theta-\sin\theta_0)\\&\quad=L_m\mathrm{c},\ m=1,2,\cdots,M-1\end{aligned}\tag{12}$$

Rewrite Eq. (12) into matrix form as

$$\boldsymbol{A}\boldsymbol{x}=\boldsymbol{b}\tag{13}$$

where $\boldsymbol{A}=\begin{bmatrix}\Delta f_1 & -f_0 d_1\\ \Delta f_2 & -f_0 d_2\\ \vdots & \vdots\\ \Delta f_{M-1} & -f_0 d_{M-1}\end{bmatrix}$, $\boldsymbol{x}=\begin{bmatrix}r-r_0\\ \sin\theta-\sin\theta_0\end{bmatrix}$, $\boldsymbol{b}=\begin{bmatrix}L_1\mathrm{c}\\ L_2\mathrm{c}\\ \vdots\\ L_{M-1}\mathrm{c}\end{bmatrix}$, $L_m=0,\pm1,\cdots,m=1,2,\cdots,M-1$.

To decouple the range and angle, the beampattern should have the unique maximum point in the range-angle distribution diagram, which means the Eq. (13) has the unique solution (θ_0, r_0). The necessary and sufficient condition of that the Eq. (13) has the unique solution is

$$\mathrm{rank}(\boldsymbol{A})=\mathrm{rank}\left(\tilde{\boldsymbol{A}}\right)=2\tag{14}$$

where rank $(\cdot)$ is the rank of a matrix, $\tilde{\boldsymbol{A}}=(\boldsymbol{A},\boldsymbol{b})$. When $\mathrm{rank}(\boldsymbol{A})=\mathrm{rank}\left(\tilde{\boldsymbol{A}}\right)=1$, the Eq. (13) has infinite solutions, corresponding to the conventional FDA condition, which will be discussed in detail later.

To satisfy rank $(\boldsymbol{A})=2$, $d_m\neq P\Delta f_m$, P is a constant.

To satisfy $\mathrm{rank}(\boldsymbol{A})=\mathrm{rank}\left(\tilde{\boldsymbol{A}}\right)$, $L_m=Qd_m$ or $L_m=S\Delta f_m$, L_m is an integer, and assume that Q, S are the minimum non-zero constants to satisfy the equations. Since $d_m\neq P\Delta f_m$ must be satisfied, the two equations cannot be hold at the same time but when $L_m=0$, $\forall m=1,2,\cdots,M$–1.

In the following, under the condition of $d_m\neq P\Delta f_m, L_m=0,\pm1,\cdots$, we make a summary with different parameter configurations:

(1) when $L_m=0$, the Eq. (13) has the unique solution (θ_0, r_0);

(2) when $L_m=Qd_m\neq0$, $L_m\neq S\Delta f_m$, the Eq. (10) has the solutions $(\arcsin(\sin(\theta_0)-kQ\lambda_0),\ r_0)$, $\lambda_0=\dfrac{\mathrm{c}}{f_0}$, $k=0,\pm1,\pm2,\cdots$. When $|\sin(\theta_0)-kQ\lambda_0|\leq1$, the angle grating lobes will occur at angle $\arcsin(\sin(\theta_0)-kQ\lambda_0)$ in the beampattern. Otherwise, the Eq. (13) has no solution, resulting in no angle grating lobes;

(3) when $L_m=S\Delta f_m\neq0, L_m\neq Qd_m$, the Eq. (13) has the $(\theta_0, r_0+Sk\mathrm{c})$, $k=0,\pm1,\pm2,\cdots$, which means the range grating lobes will occur at $r_0+Sk\mathrm{c}$ in the beampattern.

Note that in array theory, when the adjacent element spacing is less than half the wavelength, the angle grating lobes will never appear. If $Q\lambda_0=\pm1$ and $\theta_0=0°$, where the element spacing is λ_0, then the grating lobes will occur at angle $\pm90°$. But $L_m=S\Delta f_m$ can always be satisfied since L_m is an integer whose range is $[-\infty,+\infty]$. The range grating lobes will always occur at range $r_0+Sk\mathrm{c}$ in the beampattern. The position of the range grating lobe changes with different S. For example, $S=0.01$, the distance between the grating lobe and the mainlobe is 3000 km. So if $r_0\pm S\mathrm{c}$ is out of the illuminated range space $[R_{\min},R_{\max}]$, the beampattern has a single-maximum point (θ_0, r_0) in the illuminated range space, which means the range and angle are decoupled.

So we can conclude that the beampattern of the FDA is always range-periodic, the grating lobes will always occur at range $r_0+Sk\mathrm{c}$, $k=0,\pm1,\pm2,\cdots$. To obtain the single-maximum beampattern in the illuminated range space $[R_{\min},R_{\max}]$, the designing criteria for the FDA is $d_m\neq P\Delta f_m$, and $2S\mathrm{c}>R_{\max}-R_{\min}$, $|\sin(\theta_0)\pm Q\lambda_0|>1$, $k=0,\pm1,\pm2,\cdots$, $L_m=0,\pm1,\cdots$, $m=1,2,\cdots$, $M-1$, P is a constant, Q, S are the minimum non-zero constants to satisfy the equations $L_m=S\Delta f_m\neq0$ and $L_m=Qd_m\neq0$.

Once the range and angle is decoupled, the target's range and angle can be estimated directly by the FDA beamformer output. Also the 2-dementional MUSIC algorithm[16] for estimating the target's range and angle can be used as well.

2.3 Specific examples

For the conventional FDA, $\Delta f_m=m\Delta f$, $d_m=md$, Δf and d are configurable parameters to control the frequency increment and the element spacing. When $L_m=nm$, $n=0,\pm1,\pm2,\cdots$,

$m=1,2,\cdots,M-1$, we can get $\mathrm{rank}(\boldsymbol{A})=\mathrm{rank}\left(\tilde{\boldsymbol{A}}\right)=1$. Under this circumstance, the Eq. (13) has infinite solutions. The solutions form the range-angle dependent curves, which have expressions as:

$$r=\frac{f_0 d}{\Delta f}\sin\theta-\frac{f_0 d\sin\theta_0}{\Delta f}+r_0+\frac{nc}{\Delta f} \tag{15}$$

In Eq. (15), the expression is no longer related to m, which means the range-angle curve for different element coincides with each other, as depicted in Fig. 2(a). In the range-angle distribution diagram, the curve is periodic in range, and the range difference between the adjacent curves is $c/\Delta f$. The corresponding beampattern is depicted as Fig. 3(a).

For the Expf-FDA, whose frequency increment is exponentially increased, $\Delta f_m=(b^m-1)\Delta f$, $d_m=md$. b is a configurable constant. The range solution rises when b gets larger. The range-angle distribution curves and the beampattern are depicted in Fig. 2(b) and Fig. 3(b), respectively.

Likewise, for the Logd-FDA, whose element spacing is logarithmically increased, $\Delta f_m=m\Delta f$, $d_m=\log(m+1)d$. When $L_m=nm$, $n=0,\pm1,\pm2,\cdots$, $m=1,2,\cdots,M-1$, we can get $\mathrm{rank}(\boldsymbol{A})=\mathrm{rank}\left(\tilde{\boldsymbol{A}}\right)=2$, so the range grating lobes will occur in the beampattern as depicted in Fig. 3(c), and the range difference between the grating lobe and the mainlobe is $c/\Delta f$. The corresponding range-angle distribution diagram is depicted in Fig. 2(c).

For another kind of FDA, called Expf-Logd-FDA, where the frequency increment is exponentially increased and the element spacing is logarithmically increased, $\Delta f_m=(b^m-1)\Delta f$, $d_m=\log(m+1)d$. The range-angle distribution curves and beampattern are depicted in Fig. 2(d) and Fig. 3(d), respectively.

3 Simulations, Results, and Discussions

Bampattern expressed in Eq. (9) and the range-angle distribution curves expressed in Eq. (11) were simulated and plotted for different kinds of FDA discussed in Section 2. The results are discussed and compared with the different kinds of FDA. The illuminated range space is (0 km, 800 km]. To generate these plots, the values of the configurable parameters have been taken as

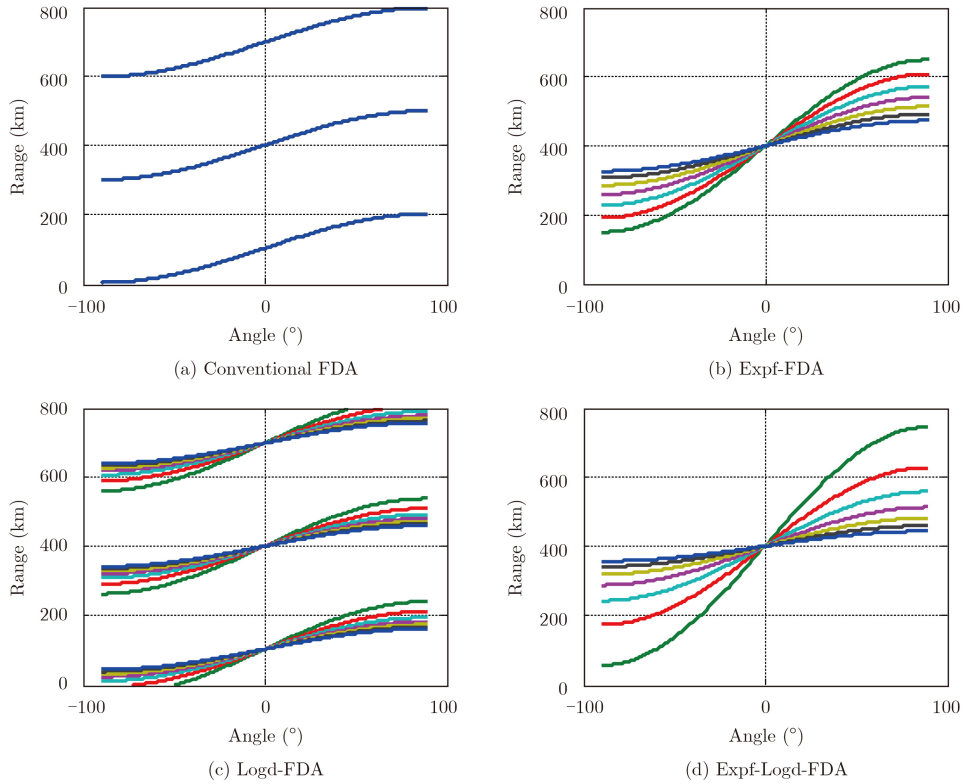

(a) Conventional FDA (b) Expf-FDA

(c) Logd-FDA (d) Expf-Logd-FDA

Fig. 2 The range-angle distribution diagram for different element

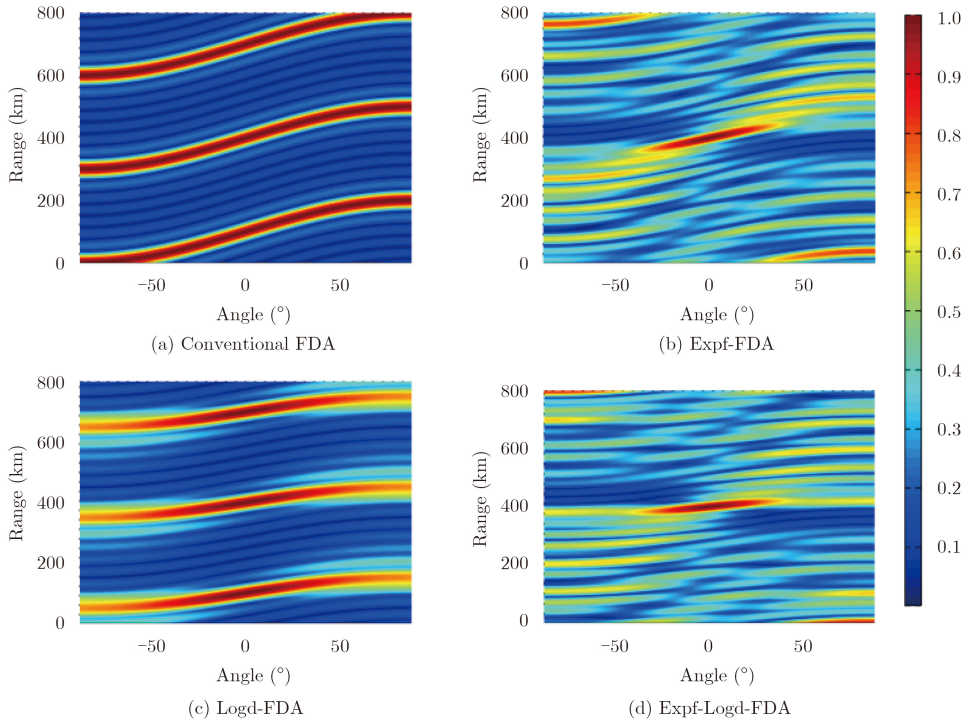

Fig. 3 Range versus angle normalized beampattern

listed in Tab. 1. To avoid angle grating lobes, the parameter d is less than half the wavelength.

Tab. 1 Parameters for simulations

Parameter	Value	Parameter	Value
Element number M	8	d	0.1 m
Reference frequency f_0	1 GHz	b	1.4
Δf	1 kHz	Desired point (θ_0, r_0)	(0°, 400 km)

The range-angle distribution curves are depicted in Fig. 2. The curves with different color represent the range-angle distribution for different elements except the reference element in the FDA. It is easy to see that the range-angle distribution of the elements are the same in conventional FDA, and the range difference between the adjacent curves is $c/\Delta f = 300$ km, which is consistent with the analysis in Section 2. For the Expf-FDA and Expf-Logd-FDA, $\Delta f_m = (1.4^m - 1)\Delta f$, the range between the first grating lobe and the mainlobe is 3e6 km, which is not in the illuminated space. So the curves of the elements in the range-angle distribution diagram have the single intersection point, which means that the beampattern has the single-maximum point in the illuminated range space. But for the Logd-FDA, when $L_m = nm$, the distance between the grating lobe and the mainlobe is $c/\Delta f = 300$ km according to the analysis in Section 2. So in the range-angle distribution diagram, the curves have 3 intersection points, the range difference between adjacent intersection points is 300 km.

The beampatterns are depicted in Fig. 3. Similar to the range-angle curve in Fig. 2, the beampattern of the conventional FDA is a range-angle-dependent beampattern. For the Expf-FDA and Expf-Logd-FDA, the beampatterns have a single-maximum point in the illuminated space corresponding to the single intersection point in the range-angle distribution diagram. For the Logd-FDA, the beampattern has 3 range grating lobes corresponding to the 3 intersection points in the range-angle distribution diagram. For the latter 3 FDAs, the contour of the beampattern is an ellipse, which is because the range-angle distribution curves are tightly distributed. The direction of the major axis of the ellipse is corresponding to the most tightness distribution direction of the range-angle distribution curves.

In the meanwhile, we analyze the range and angle solutions of different FDAs in Fig. 4. The Expf-FDA and the Exp-Logd-FDA have the same range solution, and the range solution of conventional FDA and Logd-FDA are the same. That is

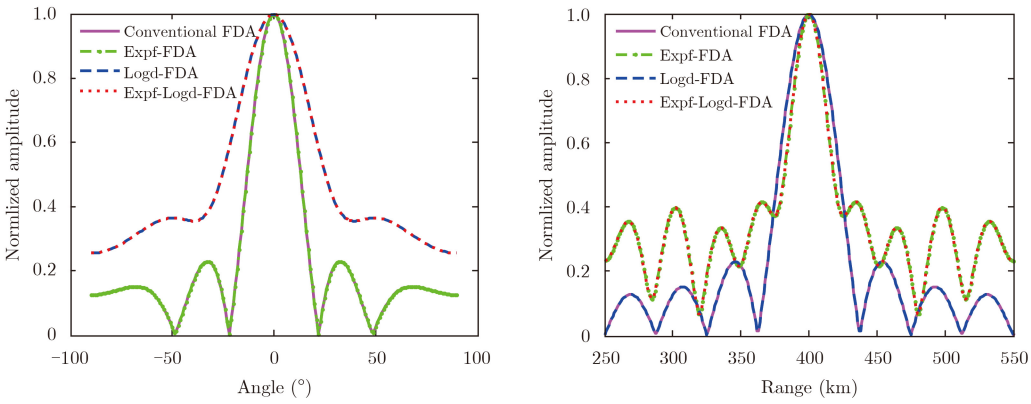

(a) Range section view (b) Angle section view

Fig. 4 Range and angle section views of beampattern

because the bandwidth across the whole array is the same for each pair. The same situation occurs for the angle solution, if the arrays have the same array aperture, they have the same angle solutions.

We choose the target position at (400 km, 20°), and the transmit beampattern is depicted in Fig. 5. Similar to Fig. 3, we can see that the single maximum beam is formed at the target position.

4 Conclusions

In this paper, we propose a basic criteria for the FDA configuration to provide a single-maximum beampattern in the illuminated space. The single-maximum beampattern can be generated by configuring the element spacing and frequency increment of the FDA. Through the analysis, we can find out that the beampattern of FDA is always range-periodic. Results show that a single-maximum beampattern can be generated with the corresponding criteria by choosing the proper frequency increment. As this paper describes the transmitter only, designing an appropriate receiver is our future work.

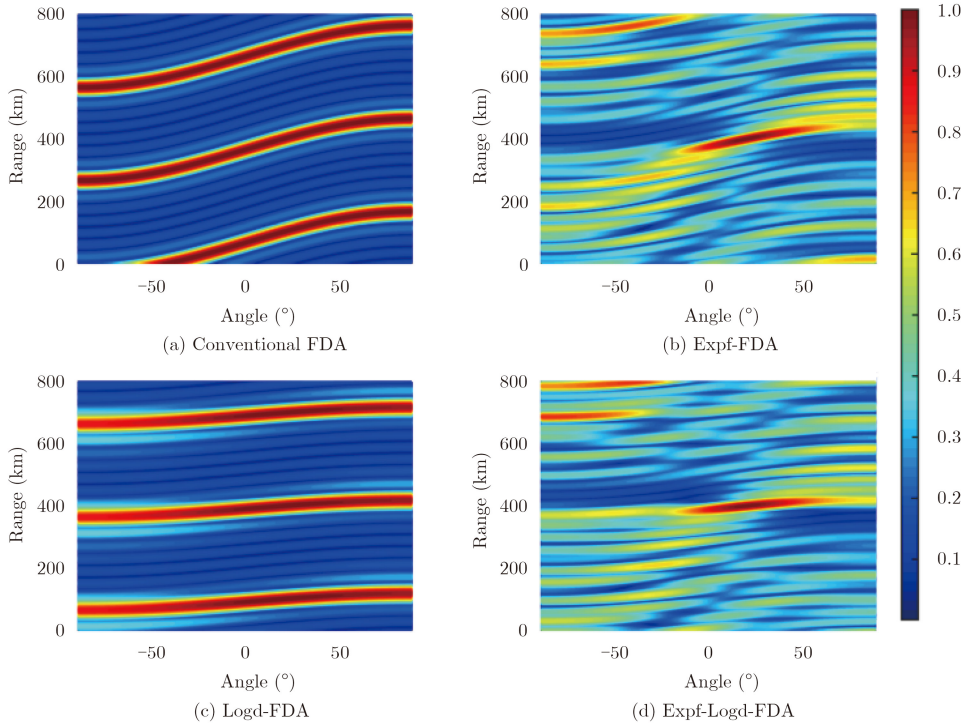

(a) Conventional FDA (b) Expf-FDA

(c) Logd-FDA (d) Expf-Logd-FDA

Fig. 5 Range versus angle normalized beampattern (target position at (400 km, 20°))

References

[1] Antonik P, Wicks M C, and Griffiths H D. Range dependent beamforming using element level waveform diversity[C]. International Waveform Diversity Design Conference, Las Vegas, NV, USA, Jan. 2006: 22–27.

[2] Secmen M, Demir S, and Hizal A. Frequency diverse array antenna with periodic time modulated pattern in range and angle[C]. IEEE Radar Conference, Boston, MA, USA, Apr. 2007: 427–430.

[3] Antonik P, Wicks M C, and Griffiths H D. Multi-mission, multi-mode waveform diversity[C]. IEEE Radar Conference, Verona, NY, USA, Apr. 2006: 580–582.

[4] Zhuang L and Liu X Z. Precisely beam steering for frequency diverse arrays based on frequency offset selection[C]. International Radar Conference, Bordeaux, France, Oct. 2009: 1–4.

[5] Chen Y G, Li Y T, and Wu Y H. Research on the linear frequency diverse array performance[C]. IEEE International Conference on Signal Processing, Beijing, China, Oct. 2010: 2324–2327.

[6] Sammartino P F, Backer C J, Griffiths H D. Frequency diverse MIMO techniques for radar[J]. *IEEE Transactions on Aerospace and Electronic Systems*, 2013, 49(1): 201–222. DOI: 10.1109/TAES.2013.6404099.

[7] Xu J W, Liao G S, and Zhu S Q. Receive beamforming of frequency diverse array radar systems[C]. 31th URSI General Assembly and Scientific Symposium (URSIGASS), Beijing, China, Aug. 2014: 1–5.

[8] Wang W Q. Range-angle dependent transmit beampattern synthesis for linear frequency diverse arrays[J]. *IEEE Transactions on Antennas Propagation*, 2014, 61(8): 4073–4081.

[9] Khan W, Qureshi I M. Frequency diverse array radar with time dependent frequency offset[J]. *IEEE Antennas and Wireless Propagation Letters*, 2014, 13: 758–761. DOI: 10.1109/LAWP.2014.2315215.

[10] Wang W Q, So H C, Shao H. Nonuniform frequency diverse array for range-angle imaging of targets[J]. *IEEE Sensors Journal*, 2014, 14(8): 2469–2476. DOI: 10.1109/JSEN.2014.2304720.

[11] Khan W, Qureshi I M, Saeed S. Frequency diverse array radarwith logarithmically increasing frequency offset[J]. *IEEE Antennas and Wireless Propagation Letters*, 2015, 14: 499–502. DOI: 10.1109/LAWP.2014.2368977.

[12] Xu Y H, Shi X W, Xu J W. Range-angle-dependent beamforming of pulsed frequency diverse array[J]. *IEEE Transactions on Antennas Propagation*, 2015, 63(7): 3262–2367. DOI: 10.1109/TAP.2015.2423698.

[13] Gao K, Wang W Q. Decoupled frequency diverse array range-angle-dependent beampattern synthesis using non-linearly increasing frequency offsets[J]. *IET Microwaves, Antennas & Propagation*, 2016, 10(8): 880–884.

[14] Gao K, Wang W Q. Transmit beamspace design for multi-carrier frequency diverse array sensor[J]. *IEEE Sensors Journal*, 2016, 16(14): 5709–5714. DOI: 10.1109/JSEN.2016.2573379.

[15] Shao H, Dai J, Xiong J. Dot-shaped range-angle beampattern synthesis for frequency diverse array[J]. *IEEE Antennas and Wireless Propagation (published online)*, 2016. DOI: 10.1109/LAWP.2016.2527818.

[16] Schmidt R O. Multiple emitter location and signal parameter estimation[J]. *IEEE Transactions on Antennas Propagation*, 1986, 34(1): 276–280.

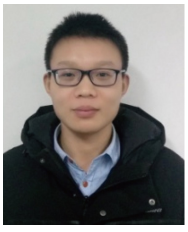

Xiang Zhe was born in Anhui, China in 1992. He received the Bachelor Degree in 2009 from Xidian University. He is currently working toward his Ph.D. degree in Signal Processing at National Laboratory for Radar Signal Processing of Xidian University. His major interests are frequency diverse radar, polarimetric radar, and interference suppression.

E-mail: xzysn152@163.com

Chen Baixiao was born in Anhui, China in 1966. He received the Master degree and the Ph.D. degree in 1994 and 1997, respectively, from Xidian University. He is a professor with National Laboratory for Radar Signal Processing of Xidian University. His research interests include array signal processing and polarimetric radar.

E-mail: bxchen@xidian.edu.cn